Electromagnetic manipulation for the anti-Zeno effect in an engineered quantum tunneling process

Lan Zhou,[1,2] F. M. Hu,[3] Jing Lu,[2] and C. P. Sun[1,*]
[1]*Institute of Theoretical Physics, Chinese Academy of Sciences, Beijing, 100080, China*
[2]*Department of Physics, Hunan Normal University, Changsha 410081, China*
[3]*Department of Mathematics, Capital Normal University, Beijing, 100037, China*
(Received 24 March 2006; published 11 September 2006)

We investigate the anti-Zeno phenomenon as well as the quantum Zeno effect for the irreversible quantum tunneling from a quantum dot to a ring array of quantum dots. By modeling the total system with the Anderson-Fano-Lee model, it is found that the transition from the quantum Zeno to the quantum anti-Zeno effect can happen by adjusting magnetic flux and gate voltage.

DOI: 10.1103/PhysRevA.74.032102 PACS number(s): 03.65.Xp, 03.65.Ta, 73.63.Kv

I. INTRODUCTION

The modern development of quantum technology enables people to control the quantum processes of a microscopic system by an external field [1–6]. From the point of view of quantum mechanics, the objective of quantum control is to reach a desired state (called the target state) from the initial state of the controlled system by manipulating its external parameters. Some aspects of quantum information can be understood as quantum control [7]. For example, quantum computation, which manipulates the evolution of a quantum system by appropriate logic gate operations, is essentially a quantum control process using external parameters. In quantum error correction, feedback control is used to detect the unwanted couplings and correct them [1]. Quantum measurement can also be regard as a special control process, which projects the unknown state into a definite state that we desire with maximized probability through wave-function collapse.

In quantum control, an intriguing concept is to use the quantum Zeno effect [8,9]. This effect freezes the evolution of a quantum state through frequent measurements. For instance, in quantum bang-bang control [1], the measurement operations are generalized by a sequence of pulses. Recently a quantum control scheme associated with an effect opposite to the quantum Zeno effect was discovered, which accelerates the decay of the unstable state by frequent measurements. This effect is called the anti-Zeno effect [10–14] or inverse Zeno effect. This discovery opens a new area for quantum control and has been used to control various physical systems, such as trapped atoms in an optical-lattice potential [15], a superconducting current-biased Josephson junction [16], ultracold atomic condensates [17], and so on.

In this paper, we consider the anti-Zeno effect with an engineered system formed by an experimentally accessible ring-type quantum-dot array and an extra quantum dot. Here, the extra dot is coupled to one dot of the array. Since it is an artificial system with more flexibly controlled parameters, we can study the dynamic details of the transition between the quantum Zeno and the quantum anti-Zeno effects in the one-directional quantum tunneling of an electron from the extra dot to the quantum-dot array. Our main purpose is to find a way of controlling the electron tunneling. Our investigation is mainly based on the discovery that the k-space representation of the quantum-dot ring model is equivalent to the famous Anderson-Fano-Lee model [18–20], which correctly describes the irreversible quantum process of a single energy level coupled with a continuous-spectrum bath. Then the standard approach [21] is used to obtain the analytic solution for the quantum tunneling dynamics. We also consider the tunneling dynamics of bosons in a one-dimensional optical lattice with the same configuration as that of fermions.

This paper is organized as follows. In Sec. II, we describe the engineered model of the quantum-dot array. Then we point out that its k-space representation is essentially the Anderson-Fano-Lee model. In Sec. III, we study the quantum irreversible process of quantum tunneling in the Heisenberg picture. In Sec. IV, we calculate the modified tunneling rate by successive projective measurements, which are performed on one dot to detect whether an electron is trapped there. We also use a numerical calculation to confirm our observations. In Sec. V, we discuss similar problems for bosons. Finally, in Sec. VI, we conclude the paper with some remarks.

II. QUANTUM-DOT ARRAY MODEL FOR ONE-DIRECTIONAL QUANTUM TUNNELING

We begin with a system of $2N$ identical quantum dots arranged in a ring threaded by a magnetic flux ϕ. Here, each structureless quantum dot traps only one electron in a single state. The sites of the quantum-dot ring are labeled by 0, 1,…, $2N-1$. The zeroth quantum dot interacts with an additional quantum dot in addition to those placed on the ring, as is illustrated schematically in Fig. 1(a).

Under the tight-binding approximation, the model Hamiltonian reads [22–25]

$$H = \hbar J \sum_{j=0}^{2N-1} e^{i\pi/N\phi} \hat{a}_j^\dagger \hat{a}_{j+1} + \hbar \omega_A \hat{a}_A^\dagger \hat{a}_A + \hbar g \hat{a}_0^\dagger \hat{a}_A + \text{H.c.}, \quad (1)$$

which describes the electron tunneling dynamics of this quantum-dot system controlled by a magnetic flux. Here, J

*URL: http://www.itp.ac.cn/~suncp. Electronic address: suncp@itp.ac.cn

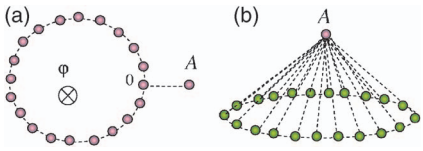

FIG. 1. (Color online) (a) The real-space schematic illustration for $2N$ identical quantum dots arranged in a ring threaded by a magnetic flux, with the zeroth dot interacting with dot A. (b) The virtual-space schematic illustration for a ring quantum-dot array coupled with quantum dot A homogeneously.

denotes the hopping integral over the jth and $(j+1)$th sites. For simplicity, we assume J is a constant. g is the coupling strength between the quantum dots at the zeroth site and the additional site A; ω_A is the on-site potential (also called the chemical potential) of site A; ϕ is the magnetic flux through the ring; and $a_j^\dagger$ (a_j) is the fermion creation (annihilation) operator at the jth site. We note here that the above Hamiltonian was presented by Peierls [22] to study the magnetic flux effect phenomenologically up to the second-order approximation.

We consider a dual picture [Fig. 1(b)] of the above quantum-dot model illustrated by Fig. 1(a). Through the Fourier transformation

$$\hat{a}_j = \frac{1}{\sqrt{2N}} \sum_{k=0}^{2N-1} e^{i\pi/Nkj} \hat{a}_k, \tag{2}$$

the original Hamiltonian is transformed into a k-space representation [26]. In this momentum representation, the Hamiltonian becomes

$$H = \hbar \sum_{k=0}^{2N-1} \epsilon_k \hat{a}_k^\dagger \hat{a}_k + \hbar \omega_A \hat{a}_A^\dagger \hat{a}_A + \frac{\hbar g}{\sqrt{2N}} \sum_{k=0}^{2N-1} (\hat{a}_k^\dagger \hat{a}_A + \text{H.c.}), \tag{3}$$

where

$$\epsilon_k = 2J \cos \frac{\pi}{N}(\phi + k) \tag{4}$$

is the well-known Bloch dispersion relation. In this dual model (3), the quantum dots in the ring-type array are coupled to the single quantum dot A homogeneously. The $2N$ modes of the ring quantum-dot array are characterized by the operators $\hat{a}_k^\dagger$ and $\hat{a}_k$, which create and annihilate a quasiexcitation in the kth mode.

From the above dual picture of the quantum-dot array model, it can be observed that a one-directional quantum tunneling in our quantum-dot model can occur as a typical quantum dissipation phenomenon. Since the quantum dot A is coupled to the other quantum dots of the ring array, the electron in this dot can easily tunnel into the array, but it is very difficult for all the electrons in the array to go back to the dot A simultaneously. Thus the electron in the quantum dot A will experience an irreversible process. A similar phenomenon was studied as the Fano model [18] for atomic physics, the Anderson model for condensed matter physics [19], and even as the Lee model for particle physics [20]. In this paper we focus on the quantum control problem for irreversible quantum tunneling, namely, we explore the possibility of changing the microscopic quantum tunneling process by adjusting the external field, since many parameters in such an artificially engineered system can be tuned to a great extent.

III. EVOLUTION DYNAMICS IN THE HEISENBERG PICTURE

The total system described by Hamiltonian (3) is isolated as a closed system, but the electron in each dot, such as dot A, is an open system. When we are only interested in the dynamics of quantum dot A, the quantum-dot array can be regarded as an engineered environment. In the terminology of the quantum open system approach, the Hamiltonian (3) describes a single-level system interacting with an environment [27]. Such an engineered environment is composed of an ensemble of $2N$ qubits. State $|1\rangle$ denotes one electron in the dot, and $|0\rangle$ denotes no electron in the dot. The unitary operator generated by the Hamiltonian (3) entangles the system with the environment.

Now we investigate the dynamics of the model (3) in the Heisenberg picture. The Heisenberg equation driven by the Hamiltonian (3) results in the following equations:

$$\frac{d}{dt}\hat{a}_k(t) = -i\epsilon_k \hat{a}_k - \frac{ig}{\sqrt{2N}}\hat{a}_A, \tag{5}$$

$$\frac{d}{dt}\hat{a}_A(t) = -i\omega_A \hat{a}_A - ig \sum_{k=0}^{2N-1} \frac{\hat{a}_k}{\sqrt{2N}}. \tag{6}$$

The motions of $\hat{a}_k$ and $\hat{a}_A$ are coupled via the coupling constant g. For convenience in the following discussions, we consider only its short-time behavior, by employing the operator ordering prescription. We should point out that the short-time behavior has been studied in Ref. [10] for the general case with the coupling of a discrete state to a continuum. With an analytical approach in the Schrödinger picture, the authors of [10] found that the decay process of a single state coupled to a discrete or a continuous spectrum is determined by the energy spread caused by the measurements [10]. Our approach will be carried out in the Heisenberg picture for the present realistic system.

Defining two fermion operators

$$\hat{C}_k = \hat{a}_k e^{i\epsilon_k t}, \quad \hat{B} = \hat{a}_A e^{i\omega_A t} \tag{7}$$

to remove the high-frequency effect, we have the integro-differential equation

$$\frac{d\hat{B}}{dt} = -\frac{ig}{\sqrt{2N}} \sum_{k=0}^{2N-1} e^{-i(\epsilon_k - \omega_A)t} \hat{C}_k(0) - \frac{g^2}{2N} \sum_{k=0}^{2N-1} \int_0^t \hat{B}(t_1) e^{i(\epsilon_k - \omega_A)(t_1 - t)} dt_1 \tag{8}$$

from the above Eqs. (5) and (6). Integrating both sides of Eq. (8), we proceed with an iteration method to obtain a suitable operator ordering prescription for the dynamic evolution of

$\hat{a}_k(t)$ and $\hat{a}_A(t)$. If the coupling strength g is small, we can omit terms with the order of g higher than 2. It is a reasonable assumption that $\hat{a}_A(t)$ varies slowly within a short time interval. By replacing $\hat{B}(t_1)$ with $\hat{B}(0)$ in the right-hand side of the above equation, the evolution of the annihilation operator $\hat{a}_A(t)$ is approximately calculated as

$$\hat{a}_A(t) = \hat{a}_A(0)e^{-i\omega_A t} - \sum_{k=0}^{2N-1} \frac{ig\hat{a}_k(0)}{\sqrt{2N}} e^{-i\omega_A t} \int_0^t e^{-i(\epsilon_k-\omega_A)t'} dt' - \hat{a}_A(0)e^{-i\omega_A t} \int_0^t dt'(t-t')e^{i\omega_A t'}\Phi(-t'), \tag{9}$$

where the memory function [16]

$$\Phi(t) = \frac{g^2}{2N} \sum_{k=0}^{2N-1} e^{i\epsilon_k t} \tag{10}$$

depends only on the quasiexcitation in the $2N$ modes of the ring quantum-dot array and the magnetic flux.

IV. QUANTUM TUNNELING AFFECTED BY A SEQUENCE OF PROJECTIVE MEASUREMENTS

Now we consider the decay of the tunneling rate induced by an instantaneous projective measurement into the initial state of the total system. Suppose that the entire system is initially prepared in a state with an electron in the quantum dot A and no electron in the ring array. Let $|0\rangle$ denote the vacuum state that no electron exists in the entire system. Then the initial state can be written as

$$|\psi(0)\rangle = \hat{a}_A^\dagger(0)|0\rangle. \tag{11}$$

Obviously, this state is unstable since the electron may tunnel to any dot of the quantum-dot array in Fig. 1(b). After a period of evolution, the probability for finding the electron inside the dot A and no electrons in the ring array is

$$p(t) = |\langle\psi(0)|U(t)|\psi(0)\rangle|^2, \tag{12}$$

where $U(t)=\exp(-iHt/\hbar)$ is the unitary operator.

Assume the coupling strength g is small. For a projective measurement into the initial state, the probability for finding the electron in the initial state is

$$p(t) = \exp(-Rt), \tag{13}$$

which decays exponentially with a decay rate R calculated as

$$R = 2\,\mathrm{Re}\int_0^t dt' G(t,t')e^{-i\omega_A t'}\Phi(-t'), \tag{14}$$

where $\Phi(t')$ is just the memory function we defined above and $G(t,t')=(1-t'/t)$. This is a similar expression to the ones obtained in Refs. [10–14].

To justify the above result, we assume the system is initially prepared in the state $|\psi(0)\rangle=\hat{a}_A^\dagger(0)|0\rangle$. The probability for finding the electron inside the dot A and no electrons in the array is $p(t)=|\langle 0|\hat{a}_A(t)|1_A\rangle|^2$. With the explicit expression Eq. (9) for $\hat{a}_A(t)$, we obtain

$$p(t) = \left|1 - \int_0^t dt'(t-t')e^{-i\omega_A t'}\Phi(-t')\right|^2. \tag{15}$$

Since g is small and $\Phi(t)$ is proportional to g^2, we approximately have

$$p(t) \approx \left|\exp\left(-\int_0^t dt'(t-t')e^{-i\omega_A t'}\Phi(-t')\right)\right|^2, \tag{16}$$

or Eq. (13) with $R(t)$ defined by Eq. (14).

After such measurements have been done $n=t/\tau$ times, the survival probability for finding the electron still in dot A is

$$\begin{aligned} p(t=n\tau) &= \exp\left(-2n\int_0^\tau dt'(\tau-t')e^{-i\omega_A t'}\Phi(-t')\right) \\ &= \exp\left(-2t\int_0^\tau dt' G(\tau,t')e^{-i\omega_A t'}\Phi(-t')\right) \\ &= \exp\left(-2t\,\mathrm{Re}\int_0^\tau dt' G(\tau,t')\Theta \times(\tau-t')e^{-i\omega_A t'}\Phi(-t')\right), \end{aligned} \tag{17}$$

which gives the decay rate modified by measurement:

$$R = 2\,\mathrm{Re}\int_0^{+\infty} dt' G(\tau,t')\Theta(\tau-t')e^{-i\omega_A t'}\Phi(-t'), \tag{18}$$

where $\Theta(x)$ is the Heaviside unit step function, i.e., $\Theta(x)=1$ for $x>0$, and $\Theta(x)=0$ for $x<0$.

Define the modulation function caused by measurement as

$$f(t) = G(\tau,t)e^{-i\omega_A t}\Theta(\tau-t). \tag{19}$$

By applying the Fourier transformation to the modulation function $f(t)$ and the memory function $\Phi(-t)$, the decay rate modified by frequent projective measurement is calculated as

$$R = \frac{g^2\tau}{4\pi N}\sum_{m=0}^{2N-1} \mathrm{sinc}^2\left[\left(J\cos\frac{(\phi+m)\pi}{N} - \frac{\omega_A}{2}\right)\tau\right]. \tag{20}$$

Equation (20) shows that the decay rate R depends on four parameters: the time interval τ between two successive measurements; the number $2N$ of quantum dots placed on the ring; the on-site-potential ω_A, which is applied to the dot A by the electrode; and the magnetic flux ϕ through the ring quantum-dot array; but only τ, ω_A, and ϕ can be adjusted experimentally.

To study the dynamic details of the irreversible quantum tunneling, we first consider the dynamic behavior of the electron with no measurement performed. The Fermi golden rule is used to calculate the decay rate as

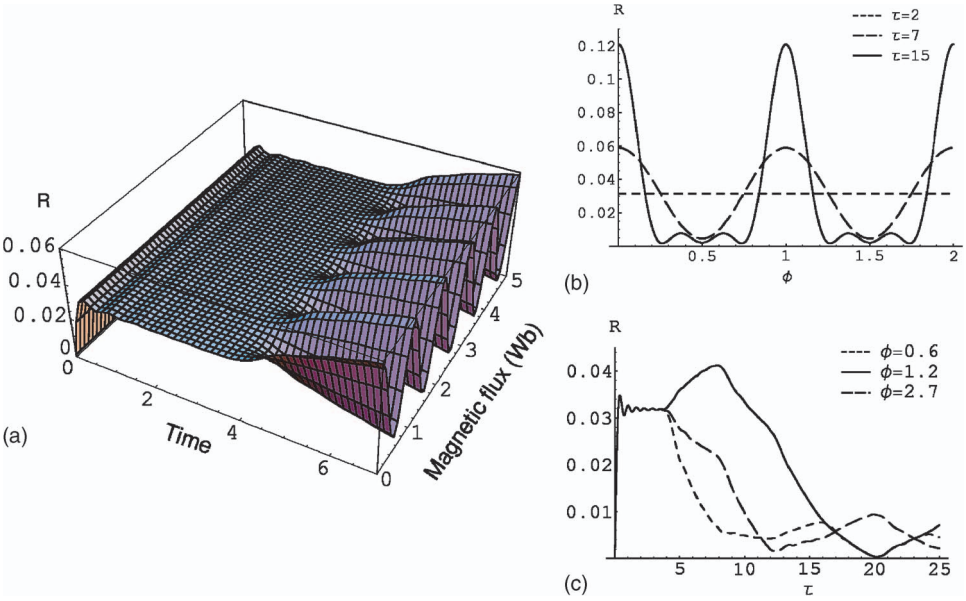

FIG. 2. (Color online) (a) Three-dimensional (3D) diagram for the behavior of the decay rate as a function of τ and ϕ under the setting $J=5$, $g=1$, $N=20$, and $\omega_A=0$. (b) The cross sections of the 3D surface for $\tau=2,7,15$. (c) The cross sections of the 3D surface for $\phi=0.6,1.2,2.7$. The figure shows that the tunneling rate can be modulated by the magnetic flux. The unit of time interval is $\hbar$ and the unit of magnetic flux is Wb.

$$R=\frac{g^2}{4N}\sum_{m=0}^{2N-1}\delta\left(2J\cos\frac{(\phi+m)\pi}{N}-\omega_A\right). \tag{21}$$

Equation (21) shows that the decay rate depends on ω_A, N, and ϕ. If $|\omega_A|\leqslant 2J$ and the number of quantum dots placed on the ring is finite, there are two situations for the electron motion when one adjusts the magnetic flux ϕ: (1) The electron tunnels into the quantum-dot array arranged in a ring and never comes back; (2) the electron stays in site A. In the following, we will explain the physical mechanism for the switch between these two situations by adjusting ϕ. The energy level of the ring quantum-dot array is discrete in Fig. 1(b), and electron tunneling between dots occurs when the discrete energy level of one dot matches that of the other dot. The magnetic flux ϕ controls the discrete energy levels of the quantum-dot array to match or not to match the energy level of quantum dot A so that the above two phenomena can occur. As the number of quantum dots placed on the ring increases, the discrete energy levels of the dot array approach each other. Thus the effect of magnetic flux ϕ becomes vanishing, and the controllable parameter is only the on-site potential ω_A. The two phenomena described above happen to the electron when $|\omega_A|$ is smaller or larger than $2J$.

Actually, as for Eq. (21), one can also use the Wigner-Weisskopf approach [21] to describe the electron dynamic evolution approximately. To this end, we first take the Laplace transformation of Eq. (8),

$$\hat{B}(s)=\frac{\hat{B}(0)}{f(s)}-\sum_{k=0}^{2N-1}\frac{ig\hat{C}_k(0)}{\sqrt{2N}f(s)[s+i(\epsilon_k-\omega_a)]}, \tag{22}$$

where

$$f(s)=s+\sum_{k=0}^{2N-1}\frac{g^2/(2N)}{s+i(\epsilon_k-\omega_a)}. \tag{23}$$

As the coupling strength g is small, the Wigner-Weisskopf approach gives the zero point of $f(s)$ [21], which results in the approximate solution

$$\hat{B}(t)=\hat{B}(0)e^{-Rt}-\sum_{k=0}^{2N-1}\frac{ige^{-Rt}\hat{C}_k(0)}{\sqrt{2N}[i(\epsilon_k-\omega_A)-R]}, \tag{24}$$

where R has the same expression as Eq. (21). So long as the Wigner-Weisskopf approximation is valid for some time interval, the above solution can correctly describe the quantum tunneling phenomenon in the coupled-quantum-dot configuration.

Next we study the dynamic behavior of the electron in quantum tunneling when $\tau\to 0$, i.e., the system is measured continuously. In this case the decay rate for the electron tunneling from quantum dot A to the quantum-dot array vanishes. This means the electron is frozen in the quantum dot A.

Then we consider the behavior of the electronic quantum tunneling with a finite time interval between two successive measurements. Due to the finiteness of the time interval, we find that only the quantum anti-Zeno effect can occur in some cases. From Eq. (20), we can see that, when one of the energy levels of the ring dot array matches that of dot A, that is, the parameters ϕ and ω_A satisfy the following equation:

$$2J\cos\frac{(\phi+m)\pi}{N}=\omega_A, \tag{25}$$

the tunneling rate is an increasing function of time interval τ. Consequently, the quantum Zeno effect occurs. When all energy levels of the array are out of resonance with that of dot A, i.e., Eq. (25) cannot be satisfied for any m, the tunneling rate is roughly a descending function of τ. Thus the quantum anti-Zeno effect occurs. Hence, when the time interval τ between two successive measurements is finite, in the region of $|\omega_A|<2J$, the occurrence of the quantum Zeno or anti-Zeno effect depends on the magnetic flux ϕ for a given on-site potential ω_A; and for a given magnetic flux ϕ, the occurrence of the quantum Zeno or anti-Zeno effect depends on the on-site potential ω_A. In the region of $|\omega_A|>2J$, only the quantum anti-Zeno effect occurs when the time interval τ is in an appropriate finite range.

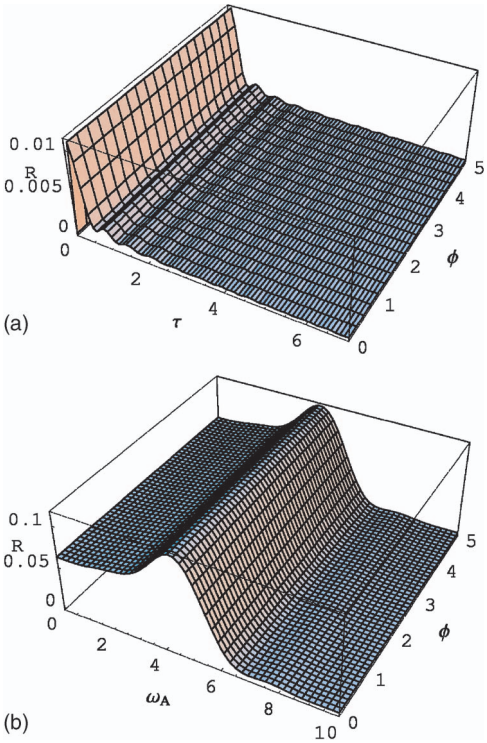

FIG. 3. (Color online) The independence of the decay rate R on magnetic flux ϕ. (a) 3D diagram for the behavior of the decay rate as a function of τ and ϕ under the setting $J=5$, $g=1$, $N=20$, and $\omega_A=20$. (b) 3D diagram for the behavior of the decay rate as a function of ω_A and ϕ under the setting $J=2.5$, $g=1$, $N=20$, and $\tau=10$.

In Figs. 2 and 3(a), we numerically plot the decay rate as a function of τ and the magnetic flux ϕ for different on-site potentials ω_A. Figure 2 is plotted when the on-site potential ω_A is just within the energy range of the ring dot array. It shows that, when the time interval approaches zero, the quantum Zeno effect does occur, which coincides with our above discussion; for a small time interval, the tunneling rate is a constant; for an appropriate time interval, whether the electron tunnels out of the quantum dot A to another dot or stays in quantum dot A is dependent on the magnetic flux. This means we can inhibit or accelerate the dissipative motion of the electron. Figure 3(a) shows that when the on-site potential ω_A is outside the energy range $[-2J,2J]$, the tunneling rate depends only on the interval τ. As $\tau\to 0$, the quantum Zeno effect also occurs, but there exists a range of finite τ, within which the system decays rapidly as the measurement frequency increases, so only the quantum anti-Zeno effect occurs. These findings verify our arguments above.

For different time intervals τ between two successive measurements, in Figs. 3(b) and 4, we numerically plot the tunneling rate as a function of the magnetic flux ϕ and on-site potential ω_A. In this system, ω_A is controlled by the electrochemical gate electrode. It can be seen that for a sufficiently small interval τ, shown in Fig. 3(b), the tunneling rate modified by measurement is independent of the magnetic flux ϕ, but for an appropriate interval τ, shown in Fig. 4, one can modulate the tunneling rate via the magnetic flux when the on-site potential ω_A is smaller then $2J$.

V. IRREVERSIBLE QUANTUM TUNNELING OF BOSONS IN AN OPTICAL LATTICE

We consider bosonic atoms trapped in a ring optical lattice [28,29], which is described as a periodic potential $V(x)=V(x+a)$ with spatial period a. In general, we can use the many-body Hamiltonian

$$H=\int \Psi^{\dagger}(x)\left(\frac{p^2}{2m}+V(x)\right)\Psi(x) + \int dx\,dy\,\Psi^{\dagger}(x)\Psi^{\dagger}(y)W(x,y)\Psi(x)\Psi(y) \tag{26}$$

to describe the quantum dynamics of a many-atom system. In the case of a dilute atomic gas, we can neglect the interaction term. When each potential well in the optical lattice is sufficiently deep, the tight-binding approximation can be used by assuming the wave function as $\Psi(x)=\Sigma_j b_j u_j(x)$, where $u_j(x)$ is localized around the site j. If we neglect the overlaps of two localized basis states that are not next neighbors, the coefficient b_j will be approximately described as a boson operator. Hence the Hamiltonian of this boson system [30–34] can be approximated as Eq. (1) with $\phi=0$,

$$H=\hbar J\sum_{j=0}^{2N-1}\hat{b}_j^{\dagger}\hat{b}_{j+1}+\hbar\omega_A\hat{b}_A^{\dagger}\hat{b}_A+\hbar g\hat{b}_0^{\dagger}\hat{b}_A+\text{H.c.} \tag{27}$$

Here, $\hat{b}_j^{\dagger}$ ($\hat{b}_j$) is the creation (annihilation) operator of bosonic atoms and the operators satisfy the commutation relations.

By Fourier transformation of the boson operators $\hat{b}_j^{\dagger}$ and $\hat{b}_j$, the boson model (27) can be transformed into a dual model similar to that of fermions [see Eq. (3)]:

$$H=\sum_{k=0}^{2N-1}\varepsilon_k\hat{b}_k^{\dagger}\hat{b}_k+\hbar\omega_A\hat{b}_A^{\dagger}\hat{b}_A+\frac{g}{\sqrt{2N}}\sum_{k=0}^{2N-1}(\hat{b}_k^{\dagger}\hat{b}_A+\hat{b}_A^{\dagger}\hat{b}_k), \tag{28}$$

where the Bloch dispersion relation is $\varepsilon_k=2J\cos(\pi k/N)$.

We now use the Heisenberg equation to study the system dynamics. By considering the short-time behavior that is described in Sec. III, we find that the evolution of the annihilation operator $\hat{b}_A$ is similar to Eq. (9):

$$\hat{b}_A(t)=\hat{b}_A(0)e^{-i\omega_A t}-\sum_{k=0}^{2N-1}\frac{ig\hat{b}_k(0)}{\sqrt{2N}}e^{-i\omega_A t}\int_0^t e^{-i(\varepsilon_k-\omega_A)t'}dt' - \hat{b}_A(0)e^{-i\omega_A t}\int_0^t dt'(t-t')e^{i\omega_A t'}\Psi(-t'), \tag{29}$$

where

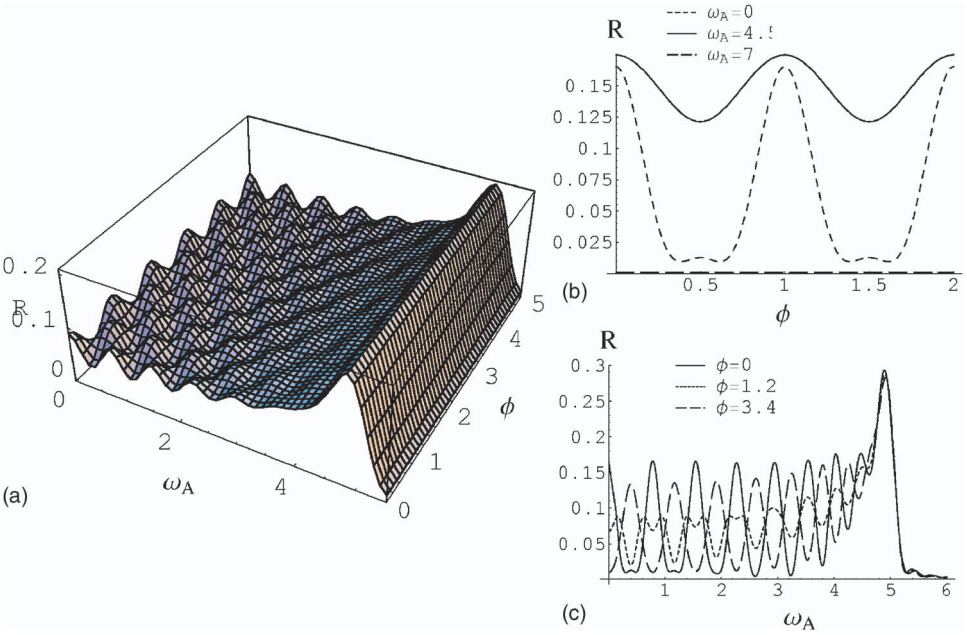

FIG. 4. (Color online) (a) 3D diagram for the behavior of the decay rate as a function of ω_A and ϕ under the setting $J=2.5$, $g=1$, $N=20$, and $\tau=10$. (b) The cross sections of the 3D surface for $\omega_A=0,4.5,7$. (c) The cross sections of the 3D surface for $\phi=0,1.2,3.4$. The figure shows that the motion of the electron can be modulated by electromagnetism.

$$\Psi(t)=\frac{g^2}{2N}\sum_{k=0}^{2N-1}e^{i\varepsilon_k t} \tag{30}$$

is the memory function [16]. Thus we can consider the decay of the atomic tunneling rate modified by an instantaneous projective measurement with respect to the initial state of the total system. Unlike fermions, there can be more than one boson in a site. Thus, in the following we will investigate the decay rate of this system with respect to three different initial states, and try to find the behavior difference between bosons and fermions.

First suppose the total system is initially prepared in a Fock state $\hat{b}_A^\dagger|0\rangle$ with only one atom in lattice site A. For M successive instantaneous projective measurements into $\hat{b}_A^\dagger|0\rangle$, the decay rate is of the form

$$\Gamma=\frac{g^2\tau}{4\pi N}\sum_{m=0}^{2N-1}\mathrm{sinc}^2\left[\left(J\cos\frac{m\pi}{N}-\frac{\omega_A}{2}\right)\tau\right], \tag{31}$$

which is exactly the fermion tunneling rate with magnetic flux $\phi=0$. It can be seen from Eq. (31) that the atomic tunneling rate depends on only three parameters: the time interval τ between two successive measurements, the number of lattice sites arranged on the ring, and the on-site potential ω_A, which is controlled by the laser intensity; but only τ and ω_A can be adjusted experimentally. When τ is very small and approaches zero, the well-known quantum Zeno effect occurs, and the system's evolution is frozen. For a finite number of sites, when τ has a finite value, the quantum Zeno and anti-Zeno effects can be switched by adjusting the laser intensity: the quantum Zeno effect occurs when the controllable variable $\omega_A=2J\cos(m\pi/N)$, and the anti-Zeno effect occurs when the on-site potential $\omega_A\neq 2J\cos(m\pi/N)$ or $|\omega_A|>2|J|$. Also, for a finite number of sites, when no measurement is performed, the system decays rapidly and the atom never goes back to site A when $\omega_A=2J\cos(m\pi/N)$ for arbitrary m; when $\omega_A\neq 2J\cos(m\pi/N)$ or $|\omega_A|>2|J|$, the system never evolves and the atom stays in site A forever. When the number of sites $2N\to\infty$, the energy of the ring array become continuous, and thus for a proper τ, the switch between the quantum Zeno and anti-Zeno effects is determined by whether $|\omega_A|$ is larger or smaller than $2|J|$.

Now we consider the case with one site containing more than one particle. Assume the initial state of this total system is a number state $|n_A\rangle$ with all n particles in site A. After time t, the probability for finding $|n_A\rangle$ is

$$p(t)=\frac{1}{n!}|\langle 0|[\hat{b}_A(t)]^n|n_A\rangle|^2. \tag{32}$$

By substituting Eq. (29) into Eq. (32), we find that after M successive projective measurements into the initial state, the probability modified by the measurements has a form similar to Eq. (16):

$$p(t)=\exp\left(-2nt\int_0^t dt' G(\tau,t')e^{-i\omega_A t'}\Psi(-t')\right). \tag{33}$$

Through defining the modulation function introduced in Eq. (19) in the energy spectra, we find that the atomic tunneling rate is n times lager than that of fermions:

$$\Gamma=n\frac{g^2\tau}{4\pi N}\sum_{m=0}^{2N-1}\mathrm{sinc}^2\left(J\cos\frac{m\pi}{N}-\frac{\omega_A}{2}\right)\tau. \tag{34}$$

The value of Eq. (34) is determined by four external controllable parameters: the time interval τ, the number of sites placed on the ring, the on-site potential ω_A, and the total number n of atoms in the entire system. The new controllable element n is added because of the boson enhancement effect. When n is large, the bosonic atoms have a strong tendency to leave site A. This just exhibits the statistical effect in quantum measurements for the localization of the boson system.

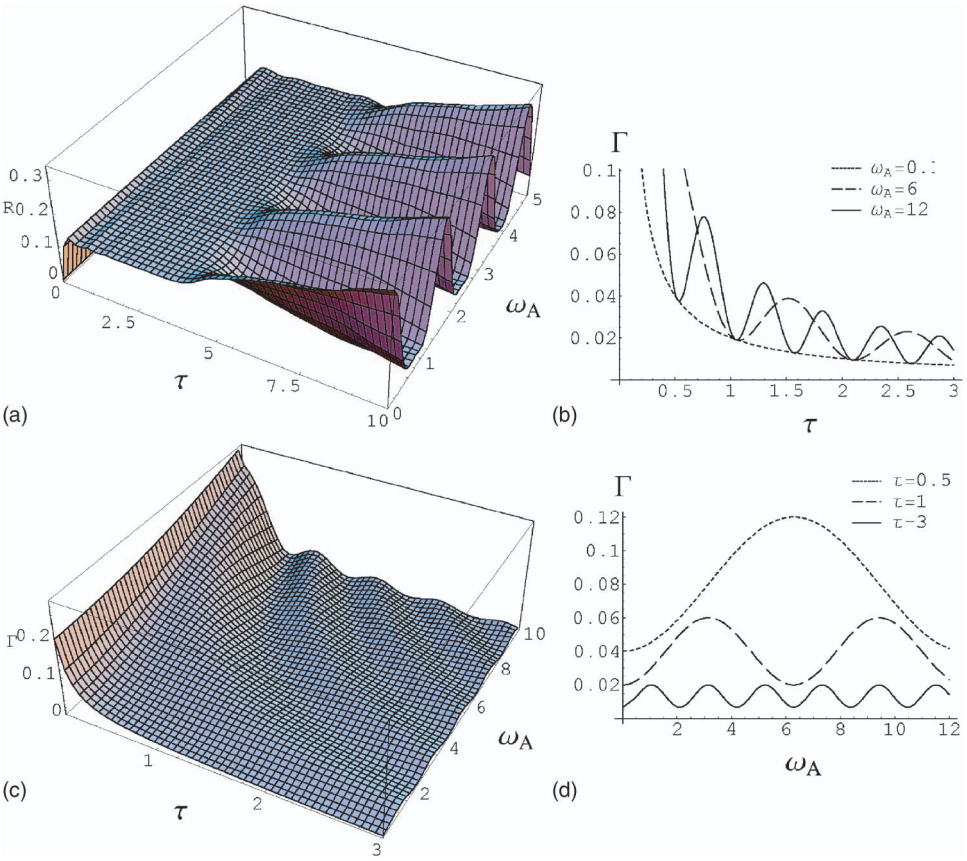

FIG. 5. (Color online) The behavior of the decay rate as a function of τ and ω_A with the system initially in a coherent state. (a) 3D diagram for a Fermi system with $J=5$, $g=2$, $N=20$, $\phi=0$. (b) 3D diagram for a Bose system with $J=5$, $g=0.01$, $N=20$, $\alpha=0.1$. (c) The cross sections of the 3D surface for $\omega_A=0.1,6,12$. (d) The cross sections of the 3D surface for $\tau=0.5,1,3$. The figure shows that the tunneling rate can be slightly modulated by the intensity of the laser beam, but overall, Γ is a decreasing function of τ for any ω_A.

Except for the n-enhanced decay of the boson atomic tunneling, the situation we discussed above is not surprising since it is very similar to that of fermions. To show the special features of boson tunneling control, we consider the case with the initial state of this total system prepared in a quasiclassical state—the coherent state $|\alpha_A\rangle=D_A(\alpha)|0\rangle$, where

$$D_A(\alpha)=e^{\alpha\hat{b}_A^\dagger-\alpha^*\hat{b}_A} \tag{35}$$

is the displacement operator. Like the Fock state listed above, this coherent state is also unstable, and the atoms at site A may tunnel to the array. Once atoms are found in one site of the array, they will spread on the array by resonant tunneling. Thus, it is difficult for all the atoms to go back to site A. In order to keep all the atoms in their original state, a sequence of measurements are performed, which project the entire system into $|\alpha_A\rangle$. A measurement projects the system into the original state with probability

$$p(t)=|e^{-|\alpha|^2/2}\langle 0|e^{\alpha^*\hat{b}_A(t)}|\alpha\rangle|^2. \tag{36}$$

To calculate the explicit expression of the above probability, we define

$$r\equiv\int_0^t dt'\left(1-\frac{t'}{t}\right)e^{-i\omega_A t'}\Psi(-t'). \tag{37}$$

As the evolution of $\hat{b}_A(t)$ was already obtained in Eq. (29), we obtain the explicit expression of the probability

$$p(t)=e^{-|\alpha|^2[|\eta(t)|^2+3-4\cos(\omega_A\tau)\eta(t)]}\times\exp\left(-\sum_m\frac{|\alpha g|^2\sin^2[(\varepsilon_m-\omega_A)t/2]}{N(\varepsilon_m-\omega_A)^2}\right), \tag{38}$$

where $\eta(t)=1-rt$. After M successive projective measurements, we find that the atomic tunneling rate Γ is modified as

$$\Gamma=\frac{|\alpha|^2}{\tau}[|\eta(t)|^2+3-2\cos(\omega_A\tau)\eta(t)-\pi r\tau^2]. \tag{39}$$

Here the expression of r is transformed into the following form through Fourier transformation:

$$r=\frac{g^2\tau}{4\pi N}\sum_{m=0}^{2N-1}\operatorname{sinc}^2\left(J\cos\frac{m\pi}{N}-\frac{\omega_A}{2}\right)\tau. \tag{40}$$

In order to study the physical phenomena with $|\alpha_A\rangle$ as the initial state, in Fig. 5, we numerically plot the decay rate as a function of two controllable external parameters τ and ω_A. The figure shows the following. (1) For a given on-site potential ω_A, as $\tau\to 0$, this unstable state decays rapidly. This phenomenon is totally different from the fermion case, where the electron is frozen in its initial state. (2) For any on-site potential ω_A, the tunneling rate can be slightly modulated by the intensity of the laser beam, but overall, it is enhanced as the measurement frequency $1/\tau$ increases. However, in the Fermi system, the crossover of the quantum Zeno and anti-Zeno effects can be controlled only by modulation of the on-site potential.

VI. SUMMARY

In conclusion, we have investigated the quantum tunneling dynamics for both fermion and boson systems in an experimentally accessible engineered configuration. In the case with electrons, the tunneling rate modified by projective measurements can be controlled by the time interval between two successive measurements, the electrochemical gate electrode, and the magnetic flux. Our results show that (1) whatever the value of the on-site potential ω_A, for vanishing time interval, the quantum Zeno effect occurs; (2) for ω_A off resonance with the energy of the dot array, the quantum anti-Zeno effect occurs as the measurement frequency increases; (3) for the on-site potential ω_A resonating with the energy of the dot array, we can inhibit or accelerate the evolution of the electron by adjusting the magnetic flux and the on-site potential. In the case of a boson system, generally, the time interval and the laser intensity control the decay of the system. The boson system shows an enhanced decay for quantum tunneling.

ACKNOWLEDGMENTS

This work was supported by the NSFC by Grant Nos. 90203018, 10474104, and 60433050, and by NFRPC by Grant Nos. 2001CB309310 and 2005CB724508. One of the authors (L.Z.) also acknowledges the support of the K. C. Wong Education Foundation, Hong Kong.

[1] L. Viola and S. Lloyd, Phys. Rev. A **58**, 2733 (1998); S. Lloyd, *ibid.* **62**, 022108 (2000).
[2] G. S. Agarwal, M. O. Scully, and H. Walther, Phys. Rev. A **63**, 044101 (2001); Phys. Rev. Lett. **86**, 4271 (2001).
[3] P. Zanardi and S. Lloyd, Phys. Rev. A **69**, 022313 (2004).
[4] Fei Xue, S. X. Yu, and C. P. Sun, Phys. Rev. A **73**, 013403 (2006).
[5] A. G. Kofman and G. Kurizki, Phys. Rev. Lett. **93**, 130406 (2004).
[6] S. Pellegrin and G. Kurizki, Phys. Rev. A **71**, 032328 (2005).
[7] V. Ramakrishna and H. Rabitz, Phys. Rev. A **54**, 1715 (1996).
[8] B. Misra and E. C. G. Sudarshan, J. Math. Phys. **18**, 756 (1977).
[9] C. B. Chiu, E. C. G. Sudarshan, and B. Misra, Phys. Rev. D **16**, 520 (1977).
[10] A. G. Kofman and G. Kurizki, Nature (London) **405**, 546 (2000).
[11] M. Lewenstein and K. Rzążewski, Phys. Rev. A **61**, 022105 (2000).
[12] A. G. Kofman and G. Kurizki, Phys. Rev. Lett. **87**, 270405 (2001).
[13] W. C. Schieve, L. P. Horwitz, and J. Levitan, Phys. Lett. A **136**, 264 (1989).
[14] A. G. Kofman and G. Kurizki, Phys. Rev. A **54**, R3750 (1996).
[15] M. C. Fischer, B. Gutierrez-Medina, and M. G. Raizen, Phys. Rev. Lett. **87**, 040402 (2001).
[16] A. Barone, G. Kurizki, and A. G. Kofman, Phys. Rev. Lett. **92**, 200403 (2004).
[17] I. E. Mazets, G. Kurizki, N. Katz, and N. Davidson, Phys. Rev. Lett. **94**, 190403 (2005).
[18] U. Fano, Phys. Rev. **124**, 1866 (1961).
[19] P. W. Anderson, Phys. Rev. **124**, 41 (1961).
[20] T. D. Lee, Phys. Rev. **95**, 1329 (1954).
[21] W. H. Louisell, *Quantum Statistical Properties of Radiation* (Wiley, New York, 1973).
[22] R. Peierls, Z. Phys. **80**, 763 (1933).
[23] S. Yang, Z. Song, and C. P. Sun, Phys. Rev. A **73**, 022317 (2006).
[24] P. Koskinen and M. Manninen, Phys. Rev. B **68**, 195304 (2003).
[25] G. Fáth and J. Sólyom, Phys. Rev. B **47**, 872 (1993).
[26] Elliott Lieb, Theodore Schultz, and Daniel Mattis, Ann. Phys. (N.Y.) **16**, 407 (1961).
[27] C. P. Sun, H. Zhan, and X. F. Liu, Phys. Rev. A **58**, 1810 (1998).
[28] L. Amico, A. Osterloh, and F. Cataliotti, Phys. Rev. Lett. **95**, 063201 (2005).
[29] X. Wang, Z. Chen, and P. G. Kevrekidis, Phys. Rev. Lett. **96**, 083904 (2005).
[30] D. Jaksch, C. Bruder, J. I. Cirac, C. W. Gardiner, and P. Zoller, Phys. Rev. Lett. **81**, 3108 (1998).
[31] Ana Maria Rey, Guido Pupillo, and J. V. Porto, Phys. Rev. A **73**, 023608 (2006).
[32] R. Bhat, L. D. Carr, and M. J. Holland, Phys. Rev. Lett. **96**, 060405 (2006).
[33] Jiannis K. Pachos, and Peter L. Knight, Phys. Rev. Lett. **91**, 107902 (2003).
[34] André Eckardt, Christoph Weiss, and Martin Holthaus, Phys. Rev. Lett. **95**, 260404 (2005).